Chemical Engineering Journal 102 (2004) 217–231

Chemical Engineering Journal

www.elsevier.com/locate/cej

On the variation of precessional flow instabilities with operational parameters in stirred vessels

L. Nikiforaki [a], J. Yu [b], S. Baldi [a], B. Genenger [b], K.C. Lee [a], F. Durst [b], M. Yianneskis [a,*]

[a] *Experimental and Computational Laboratory for the Analysis of Turbulence (ECLAT), Division of Engineering, King's College London, Strand, London WC2R 2LS, UK*

[b] *Lehrstuhl für Strömungsmechanik, Friedrich-Alexander-Universität Erlangen-Nürnberg, Cauerstrasse 4, 91058 Erlangen, Germany*

Received 16 June 2003; accepted 1 May 2004

Abstract

The effects of operational parameters such as vessel size, impeller design, diameter and blade number, Reynolds number (*Re*) and baffle number on the flows and specifically the macro-instability (MI) phenomena in stirred vessels were studied. Laser anemometry and particle image velocimetry techniques were employed to measure the mean flow and turbulence structures in vessels of diameters in the range 100–400 mm.

The data show that the characteristic frequency of the MIs, $f' = f/N$, although constant for high *Re*s, it exhibits higher value(s) over an appreciable region in the vessel for $Re < 17{,}500$. The presence of the MI is shown to broaden the measured r.m.s. levels in the vessel by up to 23%. Measurements of the tangential mean velocities near the vessel surface did not reveal any clear evidence of scaling of the flow with impeller diameter, blade number, or the number of baffles. The implications of the results for an improved understanding and a more accurate and quantitative characterisation of the flows in stirred tanks are discussed and assessed.

Keywords: Stirred vessel; Macro-instabilities; Mixing; Turbulence; Laser Doppler anemometry; Precession

1. Introduction

Mixing in chemical reactors is of immense importance for the optimisation of process and vessel design and product quality. It is responsible for dispersing and bringing reactants into contact and can strongly affect the speed of reactions. However, the complexity of mixing processes in stirred vessels renders a quantitative description of the phenomena involved rather difficult. Consequently, although mixing in stirred tanks has been extensively studied in order to elucidate the underlying physics of mass, momentum and energy transport, understanding of turbulent mixing is not yet complete. Considering also the strong impact of turbulence on process results (Kresta [1]), its accurate characterisation in stirred vessels is very important. The difficulty however, lies in the extreme complexity of the flow in a stirred tank. As Kresta [1] has pointed out, classical turbulence theories require three-dimensional instantaneous measurements of a field that is stationary, fully isotropic and in equilibrium. In reality, however, most stirred tank data comprise one-dimensional measurements of a field which is quasi-stationary, anisotropic on the larger scales of motion and locally isotropic over a limited range, fully turbulent over a limited volume and which contains additional non-random frequencies due to the blade passages. Each of these characteristics requires careful consideration before accurate quantification of the turbulence in the tank can be made.

One of the most important findings however, which further complicates the study of turbulence characteristics, is the existence of temporal mean flow variations, termed macro-instabilities (MIs), that can result in a broadening of the measured turbulence levels and therefore in erroneous interpretation of the turbulence content of the flows. Knowledge of the causes and magnitude of macro-instabilities in stirred tank reactors is very important since it may strongly influence the time scale of a particular process, as if the reaction time scale is shorter than that of the motions involved, the process will be affected and it is then essential to know what the related scales are.

Three different types of mean flow variation have been identified, with different time scales. The first kind stems primarily from changes in impeller clearance in single- or spacing in multi-impeller systems (Kresta and Wood [2];

* Corresponding author. Tel.: +44 20 7848 2428; fax: +44 20 7848 2932.
E-mail address: michael.yianneskis@kcl.ac.uk (M. Yianneskis).

1385-8947/$ – see front matter © 2004 Elsevier B.V. All rights reserved.
doi:10.1016/j.cej.2004.05.002

Nomenclature

f	macro-instability frequency (Hz)
f'	non-dimensional macro-instability frequency, $f' = f/N$
k	turbulent kinetic energy (J/kg)
r, q, z	cylindrical coordinates
u'_{BPF}	r.m.s. fluctuation due to blade passing (m/s)
u'_{MI}	r.m.s. fluctuation due to macro-instability (m/s)
u'_t	total r.m.s. fluctuation (m/s)
u', v', w'	fluctuating velocity components (m/s)
x	distance along circulation loop trajectory (m)
C, D, H, T	tank and impeller geometrical parameters indicated in Fig. 1 (m)
N	rotational speed of the impeller (Hz)
Re	Reynolds number, rND^2/m
U, V, W	mean velocity components (m/s)
Vtip	impeller tip speed (reference velocity) (m/s)

Greek symbols

μ	liquid viscosity (Pa s)
ν	kinematic viscosity (m^2/s)
ρ	density (kg/m^3)
ω	rotational speed (s^{-1})

Rutherford et al. [3], Montante et al. [4]), where depending on the clearance, an unstable state may be present with different alternating flow patterns in evidence at different times. A second flow variation phenomenon associated with changes in impeller speed (N) and/or Reynolds number (Re) has been observed in vessels stirred by pitched-blade turbines (Hockey and Nouri [5]; Distelhoff et al. [6]). The third type of macro-instability is manifested by a low-frequency mean flow variation, the magnitude, frequency (f) and origins of which are not fully understood.

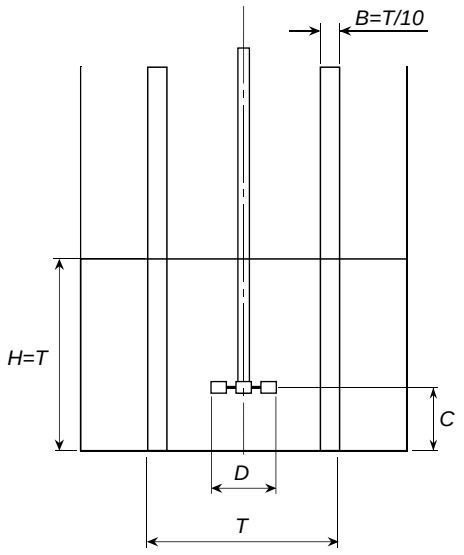

Fig. 1. Schematic diagram of stirred vessel with Rushton impeller showing main geometrical parameters.

A large number of studies have been concerned with the latter instability (Bruha et al. [7]; Montes et al. [8]; Myers et al. [9]; Hasal et al. [10], Roussinova et al. [11,12]) in an attempt to elucidate and quantify this phenomenon. Investigations with different impeller and vessel geometries have shown conclusively that mean flow instabilities are present in stirred tank flows, but although there is some agreement on the reported frequencies, the spread of the f' ($= f/N$) values determined form the published data is significant, even for geometrically similar Rushton turbine (RT) and pitched-blade turbines (PBT) (approximately 0.01–0.2). In addition, although scaling of f with impeller speed N has been reported (Montes et al. [8], Roussinova et al. [12]) different f' values have been found for low Re flows (Bruha et al. [13], Montes et al. [8]) and there is no consensus on the influence of impeller design and/or Re on f'. Recently, Nikiforaki et al. [14] studied MIs in a $T = 294$ mm vessel with a RT and a PBT of $D/T = 0.33$ and found that for $Re > 20{,}000$, a single f' value (0.015) was present for all operating conditions studied.

The approach presented in this work was formulated in order to elucidate the related phenomena and provide insight into the characteristic frequencies and variation of such instabilities for different stirred vessel configurations, in order to improve understanding of mixing processes and thus process performance, particularly as it has already been reported that such macro-instabilities may affect solid-liquid mixing (as well as single-phase blending) considerably (Bittorf and Kresta [15]). The work presented here follows on from that of Nikiforaki et al., which was limited to nominally fully turbulent Reynolds numbers and a single impeller diameter. In particular, the present work offers improved understanding of the change in f' with Re that has not been addressed to date, provides evidence of the existence of MIs over a very large range of vessel/impeller geometries, and aims to link the precessional MIs with the tangential/swirling flow in the vessels considered through detailed measurements of such flows near the top of the vessel. In the present study, a large range of experiments was carried out in vessels of different sizes, with various Res, impeller designs, clearances, number of baffles and blades in an effort to elucidate the MI phenomena and particularly the variation of f' across a vessel for different Reynolds numbers, MI effects on the measured turbulence levels and to investigate the mean flow motions obtained with different operational parameters. In view of the large number of data obtained, the substantial number of research questions stemming from the lack of understanding of MI phenomena and the need for economy of presentation, only a selection of representative results is shown, in an effort to throw

light into the issues discussed, suggest likely answers where possible and identify areas for further study where appropriate.

The experimental configurations and techniques employed are outlined in Section 2. Results obtained with first the RT and then the PBT are presented in Section 3 and the temporal and spatial characteristics of the observed mean velocity motions, macro-instability frequencies and turbulence levels are discussed, taking into account the findings of earlier investigations. In the final section, a summary of the main conclusions drawn from the work is provided, together with recommendations for future work to help elucidate further the observed phenomena.

2. Stirred vessel configurations and experimental procedures

The measurements reported in this paper were made in two different laboratories using two laser-Doppler anemometers, a particle image velocimeter and a range of vessels, Rushton turbines and pitched-blade turbines. The configurations studied are summarised in Table 1.

A characteristic diagram of the geometry of the 294 mm vessel with the Rushton impeller is shown indicatively in Fig. 1. Measurements in the 100 and 294 mm tanks were obtained with de-ionised water as the working fluid, while in the 400 mm tank with an oil of density 1021 kg/m^3 and viscosity 16.4 mPa s at 21 °C.

The two-dimensional PIV system employed for the 100 mm tank measurements is described in more detail by Baldi et al. [16]. The sampling rate was selected so that the Nyquist criterion was satisfied for all MI frequencies encountered, and the results of experiments with the highest possible frequencies were confirmed through comparisons with LDA data obtained at rates of 1–2 kHz. The LDA system employed for the 294 mm tank measurements comprised a single-channel forward scatter anemometer with a BSA processor. The measurement accuracy was 1–2% for the mean velocity and 2–5% for the turbulence level measurements.

Measurements in the 400 mm tank were obtained with a backscatter single-component anemometer with a TSI frequency counter. The working fluid (oil) for the measurements in the 400 mm tank was selected to achieve refractive-index matching with the test section walls and thus ensure extensive and unimpeded optical access throughout the flowfield. The measurement errors were around 2–3% for the mean velocity and 5% for the turbulence level values. Detailed descriptions of the related apparatus and measurement procedures are provided by Yu [17].

Most of the LDA results in the 294 mm vessel were obtained with a free surface, but some data were also obtained with a lid and confirmed that the phenomena studied were not affected to any significant extent by the presence or absence of the lid. For each measurement location, the recording time of the instantaneous signal was about 15 min. Experiments showed that the sampling time is important to have an accurate description of macro-instabilities. Zhou [18] reported that the sampling time must be long enough to cover at least 80 blade passages, i.e. for a 6-blade impeller rotating at 250 rev/min, the sampling time should be no less than 3.5 s. On the other hand, accurate study of a low-frequency phenomenon in the flow, where, according to the literature, f is of the order of 0.5 Hz, suggests a signal sampling time significantly longer than those used in many other LDA studies.

Great care was exerted in the determination of the instability frequencies obtained from the velocity-time recordings with FFT and other techniques. The problems and pitfalls involved in the identification of such frequencies have been discussed in detail by Nikiforaki et al. [14] and are not repeated here. In particular, the frequency resolution, sampling time and other processing and data acquisition parameters may have important effects on the detected spectral peaks, as does the spectral representation employed because logarithmic plots tend to show the energy contained in low frequency peaks spread out over a wide range and may lead to underestimation of the importance of such low frequencies. Consequently, all such results are presented here through linear spectra plots extensively tested for sensitivity to the aforementioned parameters. The frequency resolution employed in the FFT analysis varied from 0.006 to 0.018 Hz,

Table 1
Stirred tank configurations investigated

T (mm)	D/T	Impeller design (no. blades)	C/T	No. baffles	N (rev/min)	Re (working fluid)	Technique
100	0.33	RT (6)	0.5	4	878–2165	16,000–40,000 (water)	PIV
294	0.33	RT (6)	0.33	4	100–350	16,000–56,000 (water)	LDA
294	0.33	PBT (6, 60°)	0.33	4	100–350	16,000–56,000 (water)	LDA
400	0.225	RT (6)	0.33	4	613	5,100 (oil)	LDA
400	0.33	RT (6)	0.33	4	300	5,400 (oil)	LDA
400	0.45	RT (6)	0.33	4	150	5,000 (oil)	LDA
400	0.65	RT (6)	0.33	4	85	6,000 (oil)	LDA
400	0.33	RT (6)	0.33	2	250	4,500 (oil)	LDA
400	0.33	RT (2)	0.33	4	300	5,400 (oil)	LDA
400	0.33	RT (3)	0.33	4	300	5,400 (oil)	LDA
400	0.33	RT (4)	0.33	4	300	5,400 (oil)	LDA

to enable capturing accurately the lowest MI frequencies encountered, which were an order of magnitude higher. Similarly, sampling times corresponding to up to 80 MI cycles were employed in the measurements to ensure sufficient statistical representation of the phenomena studied.

Measurements were obtained in great detail (across the flowfield, in steps of 1–4 mm) in the 400 mm refractive index matched vessel and in numerous locations around the impeller and in the bulk flow in the 294 mm vessel. Flow visualisation results indicated that the instabilities were more pronounced and more clearly defined with the Rushton impeller, and the region near the water surface was selected for more extensive study to relate the LDA and visualisation data. For economy of presentation, only characteristic results from the experiments made in the different size vessels, with different impellers and working fluids are presented in the following sections.

3. Results and discussion

3.1. Phase-resolved mean flow field with Rushton turbine

In order to facilitate the understanding of the macro-instability phenomena investigated and discussed in the following text, it is instructive to consider first the phase-resolved mean velocity distribution in a stirred vessel. The velocity vector distribution in a vertical (r–z) plane located mid-way between two baffles in the $T = 400$ mm vessel stirred by a $D = T/3$ Rushton turbine at $C = T/3$ is shown in Fig. 2. The impeller rotational speed was 300 rev/min and the working fluid was oil ($Re = 5400$). The length of each vector indicates the velocity magnitude normalised by V_{tip} and the colour indicates the turbulence kinetic energy normalised by V_{tip}^2, with colour values shown on the right of the figure.

The double-loop mean flow pattern characteristic of this configuration can be clearly seen, with higher k values in the impeller stream, gradually decreasing with distance from the blades. It is worth noting that at this relatively low Re, the normalised k levels are similar to those obtained in earlier works with higher Re of around 40,000 (see, for example [4]). For $z/T > 0.8$ velocity magnitudes are much smaller than in the remainder of the vessel and k values are in general less than 0.01 V_{tip}^2. Earlier works with either a RT (Haam et al. [19]) or a PBT (Montes et al. [8]) have shown that it is in this region that the precessing motion of a swirling vortex that is associated with the macro-instability phenomenon can be more clearly discerned.

To illustrate the motion at a z plane near the surface ($z/T = 0.75$), the phase-resolved mean velocity vectors and the corresponding k distribution shown by the vector colours are presented in Fig. 3. The impeller rotates in a clockwise direction as viewed from the top of the vessel. The superimposed black lines have been drawn to help indicate the mean flow motion in this plane. It can be seen that the flow

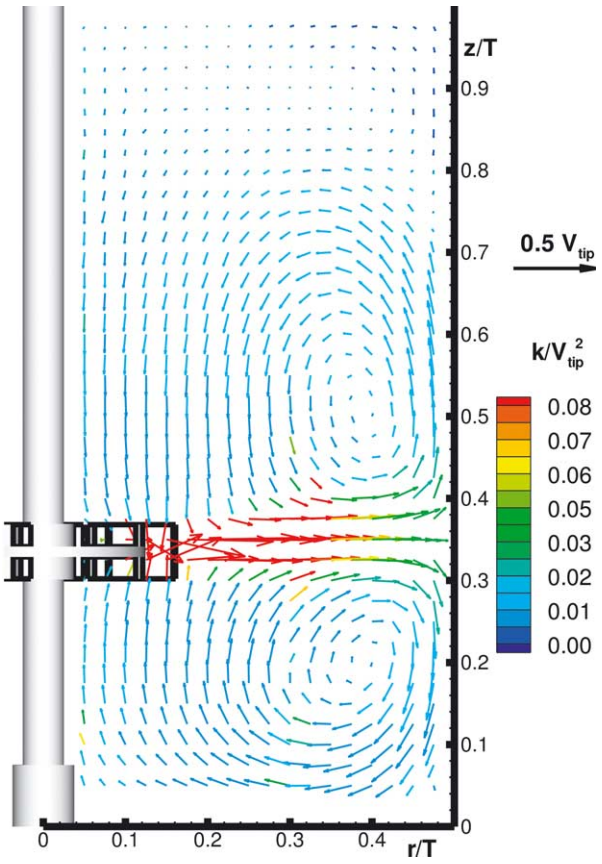

Fig. 2. Phase-resolved mean velocity vector and turbulence kinetic energy distribution at a plane midway between two baffles. Rushton turbine, $T = 400$ mm, $C/T = 0.33$, $D/T = 0.33$, $N = 300$ rev/min, $Re = 5400$.

is essentially unidirectional, with small vortices located behind each baffle. The direction of the rotational motion is from the vessel periphery and the baffles towards the region above the impeller.

The last observation and the related flow visualisation experiments concur with the observation of Guillard et al. [20], albeit for a flow stirred by two RTs, that a coherent, large scale structure may be present travelling towards the centre of the tank in its upper part, before being entrained by the flow created by the impeller.

3.2. Macro-instability frequencies with Rushton turbine

As the LDA data rate was higher with the forward-scatter LDA system employed for the 294 mm tank measurements, this set of data was used to extract most of the information on MI frequency values. Extensive frequency measurements across the 294 mm vessel with the $D = T/3$ RT located at $C = T/3$ showed clear peaks in the velocity spectra at f' around 0.02, with evidence of some harmonics at higher values. Characteristic time-resolved velocity variations and the corresponding spectra are shown in Fig. 4 for $N = 300$ rev/min ($Re = 48{,}000$) and in Fig. 5 for $N = 200$ rev/min ($Re = 32{,}000$). In both cases, cyclic

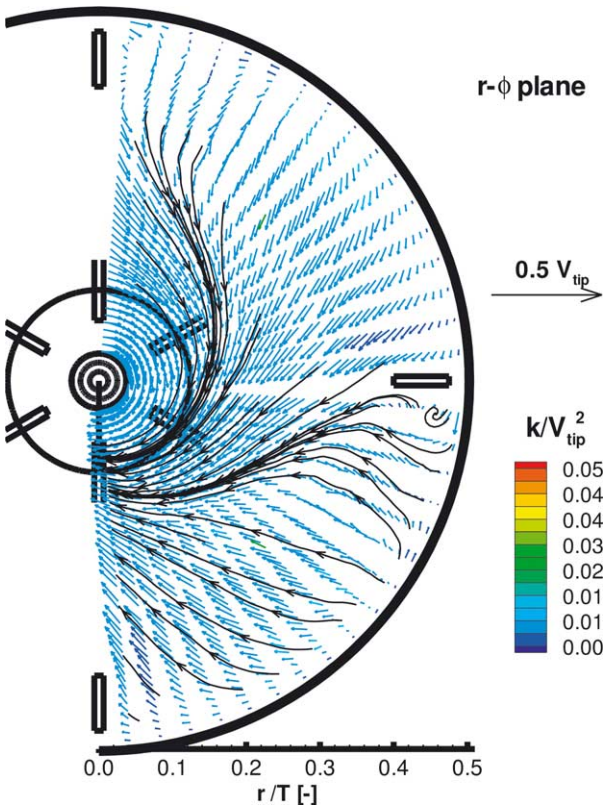

Fig. 3. Phase-resolved mean velocity vector and turbulence kinetic energy distribution at the horizontal plane $z/T = 0.75$. Rushton turbine, $T = 400$ mm, $C/T = 0.33$, $D/T = 0.33$, $N = 300$ rev/min, $Re = 5400$.

variations are evident, although not easily discernable at the time scale shown, in the velocity-time recordings. The spectra, on the other hand, provide very clear evidence that most of the macro-instability energy is concentrated in the peaks corresponding to $f' = 0.015$–0.02, with much smaller peaks present at harmonic frequencies. These f' values are identical to those reported by Nikiforaki et al. [14].

Although the 294 mm tank measurements were made for high *Re* values, it is interesting to consider the extent of the flow that is fully turbulent under lower *Re* conditions. This is important, as Bittorf and Kresta [15] have shown conclusively that the extent of active circulation in stirred vessels, even for nominally fully turbulent *Re* values, is often limited to around two-thirds of the vessel volume; consequently, nearer the top of the vessel laminar or transitional flow conditions may prevail. For this reason, measurements obtained at $Re = 5400$ in this vessel were compared with similar ones obtained in the $T = 294$ mm with water as the working fluid at $Re = 48{,}000$. In and around the impeller stream, both the normalised mean velocities and turbulence level values were similar, to within the precision of the measurements (<0.01 V_{tip}). Schäfer et al. [21] have also shown that the flow near a pitched-blade turbine (PBT) is turbulent and dynamically similar for $Re > 5000$. Far away from the impeller, however, this level of scaling is not achieved, as will be discussed further later, and it is likely that, in agreement with Bittorf and Kresta, the flows there are not fully turbulent.

A question that should therefore be posed is whether the characteristic frequency of the macro-instability varies across a vessel if fully turbulent conditions are not present throughout the vessel. This can be further complicated by the fact that often more than one precessing vortex is present, with different vortices generated at different instances and/or originating from different baffles, as was observed in the flow visualisation in the present work, especially for the flow generated by a PBT.

In order to determine the spatial distribution of f' near the top of the vessel, the PIV technique was selected. The selection of a RT located at $C/T = 0.5$ was made, as flow visualisation showed that the MI phenomenon is more clearly in evidence at this higher clearance and the associated precessing vortex motion is much better defined than with lower clearances or with a PBT. Measurements were made at a vertical plane located mid-way between two baffles in the 100 mm vessel, for $Re = 16{,}000$–$40{,}000$. Contours of the f' distribution are shown for $z/T = 0.85$–1 in Figs. 6(a)–(f).

It can be seen that at the lowest *Re* (16,000, Fig. 6 (a)), f' is around 0.015 over half of the area, but a large region with f' varying from 0.04–0.15 is present. It must be noted that the interpolation used in the contour plot may result in intermediate values of f' being displayed, but what cannot be in doubt is the presence of high f' values around $r/T = 0.15$–0.2 across the region. As *Re* is increased to 17,500, the region with high f' values is substantially decreased (Fig. 6 (b)), and this region and the corresponding maximum f' value recorded, become smaller with increasing *Re* in Figs. 6 (c)–(e). For $Re = 33{,}200$ (Fig. 6 (e)), the vast majority of the area shown exhibits f' values of around 0.01–0.02, while for the highest *Re* studied, 40,000, Fig. 6(f), $f' = 0.01$–0.02 with only a tiny area exhibiting values of 0.03–0.04. The PIV results were confirmed by f' measurements obtained with LDA in the 294 mm tank with the RT at $C/T = 0.5$ that also yielded $f' = 0.015$–0.02 at $Re = 48{,}000$ near the top as well as in the remainder of the vessel. The above findings have two important implications. First, although they confirm the f' value of 0.015 established by Nikiforaki et al. [14], they also indicate a change in MI frequency with decreasing *Re*. Second, they provide evidence that for the larger *Res* f' scales with vessel diameter for the 100 and 294 mm vessels studied here.

3.3. Macro-instabilities with pitched-blade turbine

Measurements were also obtained with a PBT to establish to what extent impeller design affected the macro-instability phenomena. The selection of the RT for the work described so far was made because the MI phenomena studied were even more complex in the case of the PBT. With this impeller, a nearly random formation and break-up of the precessional vortical motions was observed, which resulted in

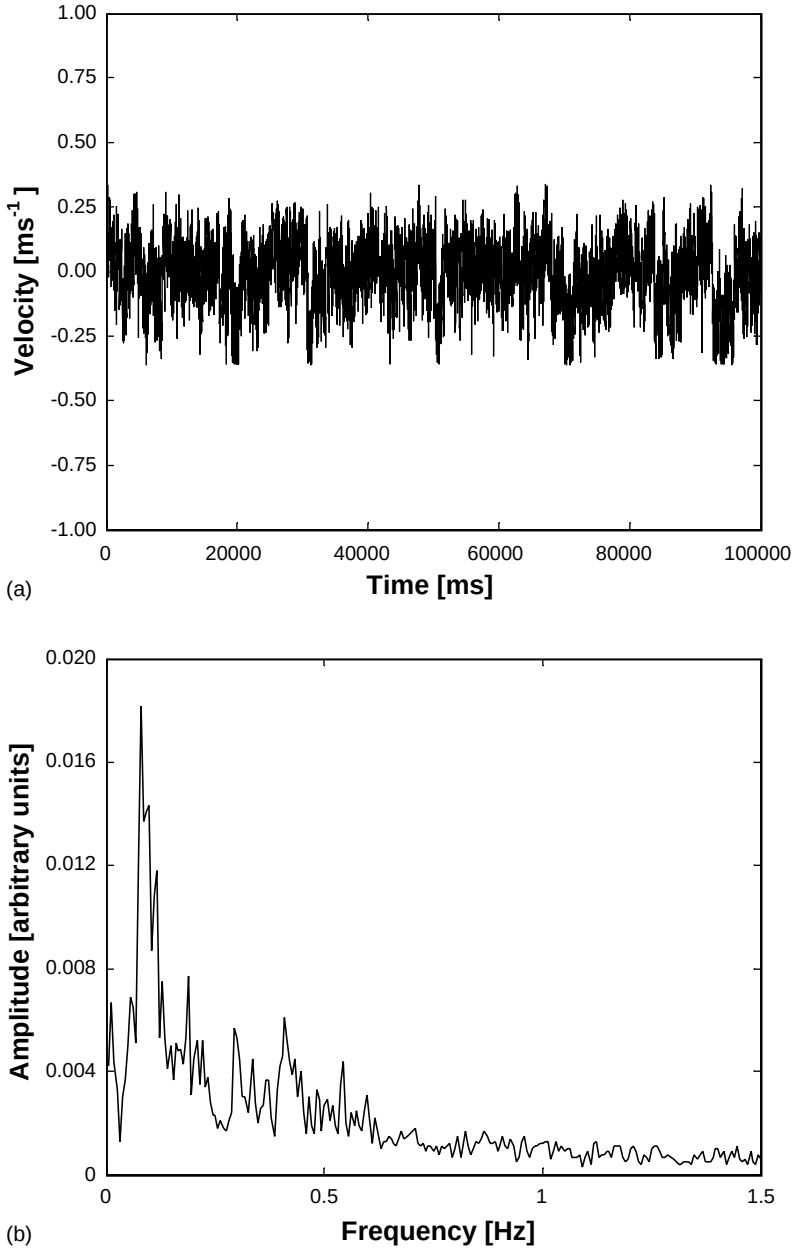

Fig. 4. Rushton turbine, $T = 294$ mm, $C/T = 0.33$; $z/T = 0.88$, $r/T = 0.11$ and $N = 200$ rpm (a) radial velocity time recording; (b) frequency spectrum of (a).

a number of frequency peaks being exhibited by the spectra, albeit all at harmonic frequencies of the lowest one. For example, in Fig. 7(a) the spectra of the velocity recordings for a speed $N = 350$ rev/min at the radial location $r/T = 0.13$ can be seen for three different axial positions $z/T = 0.22$, 0.27 and 0.4. They are all characterised by a pronounced low-frequency peak at $f = 0.1$ Hz ($f' = 0.017$) and its harmonics which in general are less pronounced. When a lower speed (150 rev/min) was used (Fig. 7(b)) the frequency spectrum was shifted to the left with the pronounced low-frequency peak corresponding to $f' = 0.015$; the spectra for lower speeds also had more defined peaks and fewer harmonics compared to those for the higher speeds. Therefore, no difference in f' could be identified with the $D/T = 0.33$ RT and PBT cases.

3.4. Effect of macro-instabilities on turbulence levels with pitched blade turbine

As mentioned earlier, the mean flow variation stemming from the macro-instabilities may result in broadening of the measured turbulence levels, if it is not accounted for. This effect has similarities to the broadening resulting from the periodicity of the flow near the impeller blades identified previously by Yianneskis et al. [22]. In order to quantify the amount of broadening of turbulence levels that might be

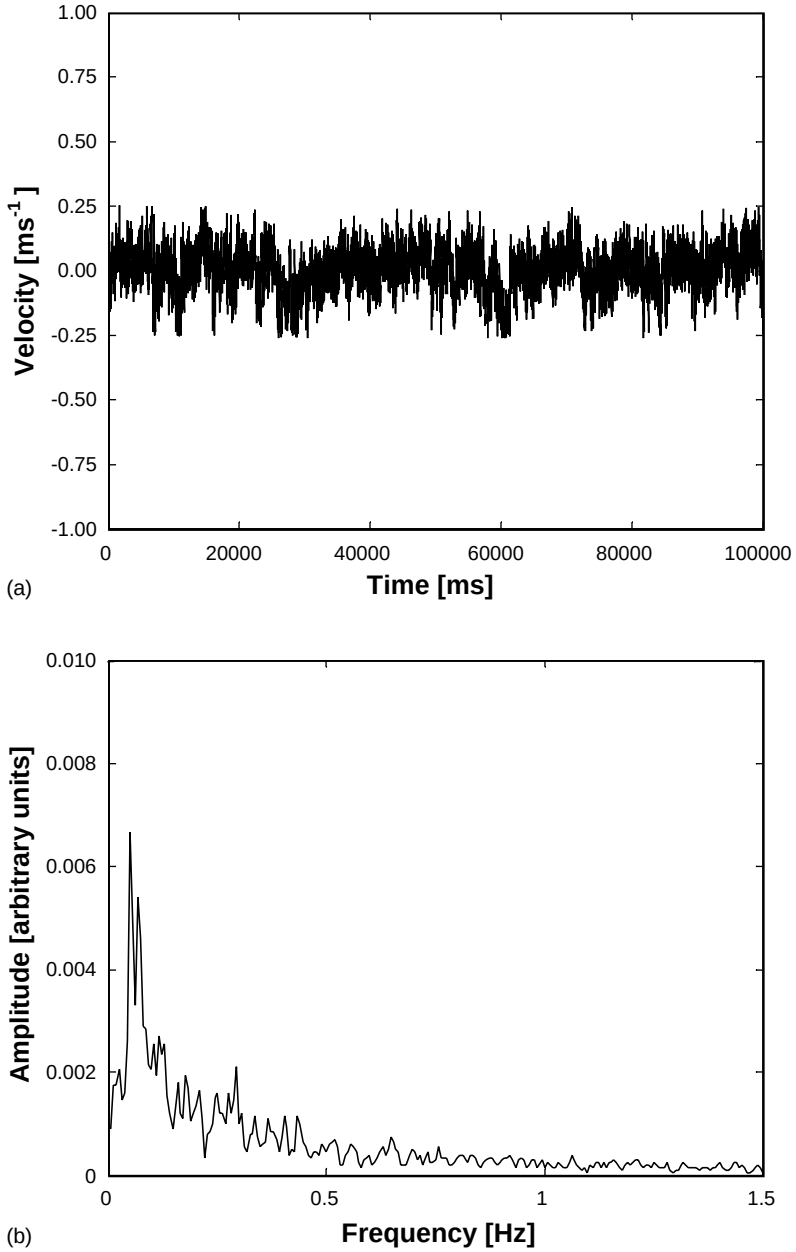

Fig. 5. Rushton turbine, $T = 294$ mm, $C/T = 0.33$; $z/T = 0.92$, $r/T = 0.11$ and $N = 300$ rpm (a) radial velocity time recording; (b) frequency spectrum of (a).

expected, the LDA data was analysed to compare the turbulence levels obtained as ensemble-averages over 360° of revolution u'_t with the corresponding values when the blade passage frequency (BPF) contribution u'_{BPF} and the corresponding macro-instability contribution u'_t are subtracted based on the following velocity decomposition of the instantaneous velocity:

$$U = \bar{U} + u + u_{\mathrm{BPF}} + u_{\mathrm{MI}}$$

where U is the instantaneous velocity, $\bar{U}$ is the time-averaged (mean) velocity, u is the randomly fluctuating component of the velocity, u_{BPF} is the regular periodic component due to the blade passages and u_{MI} is the macro-instability component. Results obtained only with the PBT are shown in this section, for brevity and as the trends with the RT were similar.

Frequencies related to the blade passages were well defined and consisted of the frequency of the blade passage (f_{BP}), the shaft rotational frequency ($f_{\mathrm{s}} = f_{\mathrm{BP}}/6$), higher harmonics and linear combinations of these frequencies (in accordance with the findings of Kovács et al. [23]), as can be seen in the velocity recording shown in Fig. 8, taken at $z/T = 0.27$, $r/T = 0.13$ for a speed $N = 350$ rev/min.

Hockey [24], experimenting with the same impeller and vessel geometry, attempted to quantify the effect of the periodic nature of the mean flow on the 360° r.m.s. value

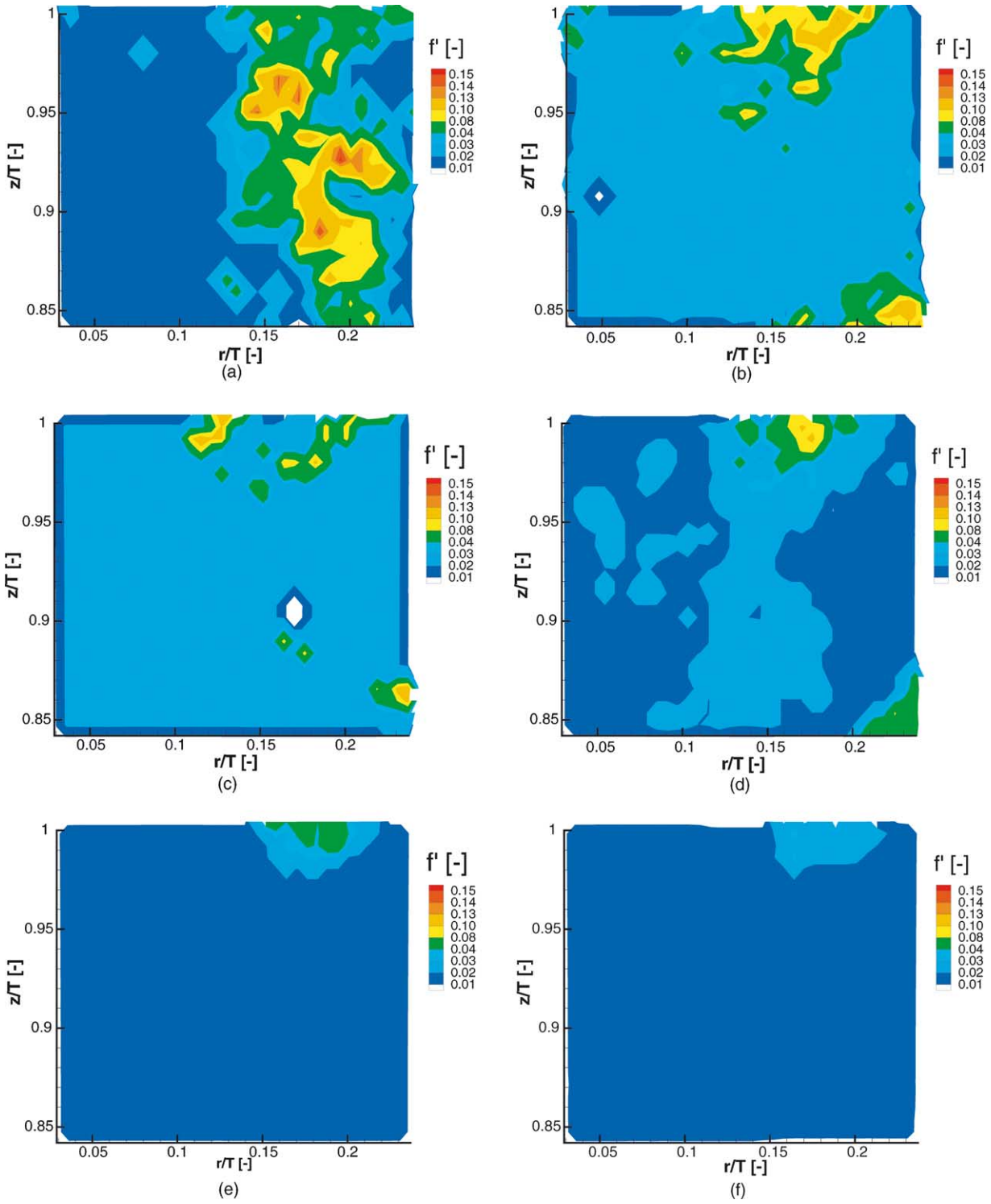

Fig. 6. Contours of the distribution of the non-dimensional macro-instability frequency f' for the Rushton turbine, $C/T = 0.5$, $T = 100$ mm, water. (a) $Re = 16{,}000$; (b) $Re = 17{,}500$; (c) $Re = 20{,}000$; (d) $Re = 26{,}600$; (e) $Re = 33{,}200$; (f) $Re = 40{,}000$.

or total r.m.s. level. Performing ensemble averaged measurements over 360° and over 1.08° intervals of impeller rotation, he estimated both the random r.m.s. velocity and the r.m.s. of the periodic component, but did not separate the MI contribution. Hockey showed that the effect of the periodic component varied depending on the position and on the component of velocity. In particular, the effect of the periodicity on the total r.m.s. values of the axial and tangential components was found to be relatively small, increasing the random r.m.s. values by about 0.03 V_{tip}. Specifically,

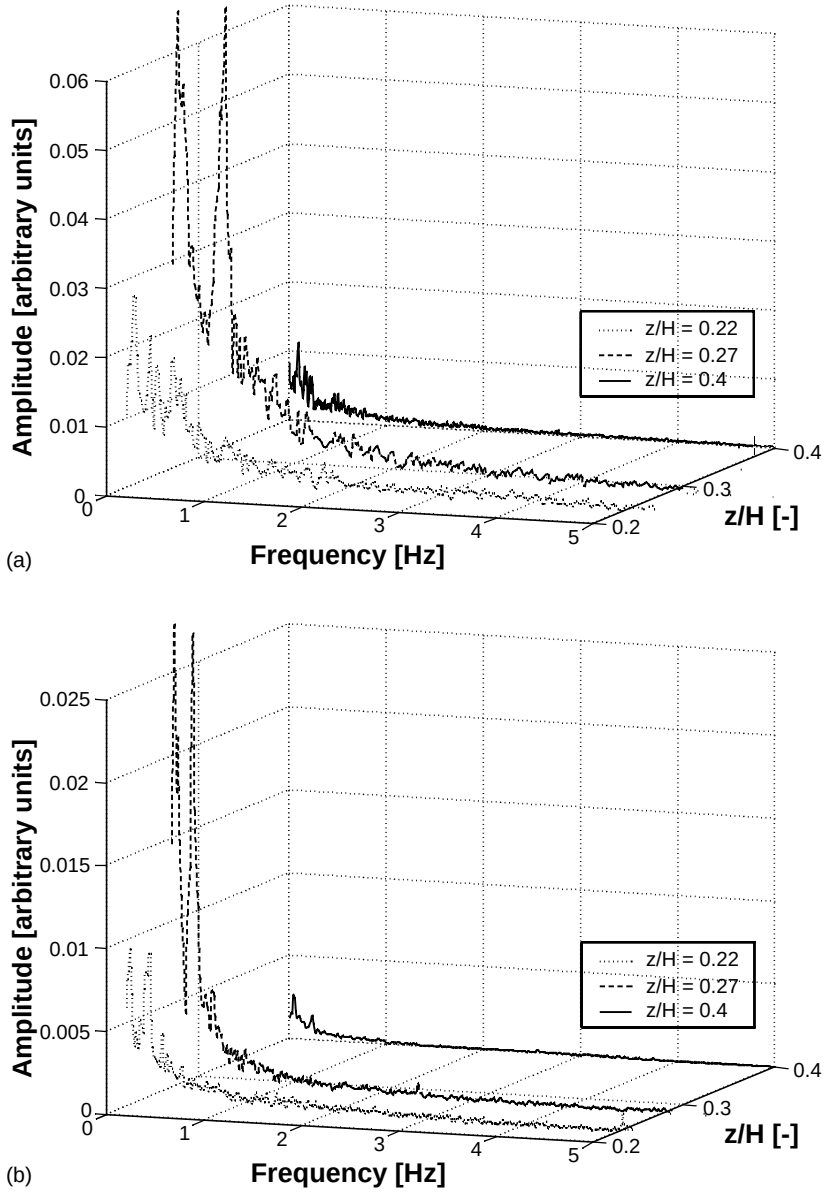

Fig. 7. Pitched-blade turbine, $T = 294$ mm, $C/T = 0.33$, $r/T = 0.13$, $z/T = 0.22$, 0.27 and 0.40. Frequency spectra of instantaneous velocity recordings for: (a) $N = 350$ rpm; and (b) $N = 150$ rpm.

measurements of the axial velocity component below the impeller ($z/T = 0.28$) showed that for $r/T = 0.06$–0.17, there was a 2–12% difference between the total r.m.s. velocity (measured with respect to the tank) and the r.m.s. velocity measured with respect to the impeller. Similar results were obtained in the present work. For the radial component, however, the r.m.s. values due to the periodic mean flow increased the total r.m.s. values by up to $0.13V_{tip}$ or more than 50% of the random value. For all velocity components though, the r.m.s. due to the periodic mean flow was nearly zero for radial locations $r/T > 0.17$, and did not affect the total r.m.s. values outside the impeller stream.

Kresta and Wood [2], experimenting with a 45° pitched-blade turbine, used a notch filter to remove the blade passage frequency from the integral of the autocorrelation function and reported no difference on the value of the integral time scale. A notch filter was also considered at first for this work to eliminate the macro-instability frequency, however, due to the fact that the MI does not occur at a single/discrete frequency, the width and the sharpness of the filter can have a strong impact on the results (Grgic [25]). For this reason, a moving window averaging technique was considered instead, and applied to the signal from which blade passage effects had been already removed.

This smoothing technique used short time averages in the time domain to smooth the signal and isolate the macro-instability, and has already been employed by Roussinova et al. [11] with a satisfactory degree of suc-

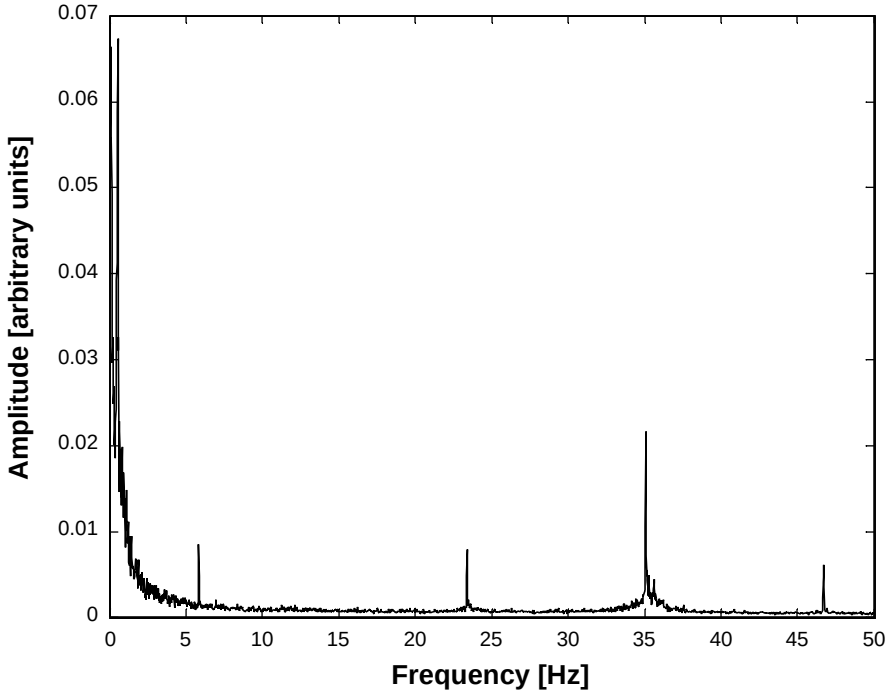

Fig. 8. Pitched-blade turbine, $T = 294$ mm, $C/T = 0.33$, $r/T = 0.13$, $z/T = 0.27$. Frequency spectrum of instantaneous axial velocity recording for $N = 350$ rpm.

cess. The parameters of the smoothing technique that needed to be adjusted were the length of the window and the number of repetitions of the smoothing process. The smoothing was considered to be complete when the low-frequency variation of the macro-instability was recovered without the presence of any higher frequency fluctuations.

The smoothed low-frequency MI signal was then subtracted from the filtered signal, and the r.m.s. of the difference represented the portion of the total r.m.s. that was due to the real turbulence ($u'_t - u'_{BPF} - u'_{MI}$). It should be carefully noted that $u'_t - u'_{BPF} - u'_{MI}$ denotes not a simple subtraction, but a proper decomposition of the r.m.s. values.

In order to quantify the broadening of the r.m.s. velocity due to the macro-instabilities the percent error due to the long time scale MI was defined in accordance with Roussinova et al. [11] as

$$\%\varepsilon_{MI} = \frac{u'_t - (u'_t - u'_{MI})}{(u'_t - u'_{MI})} \times 100\% \quad (1)$$

The error varies from 6–23% as it can be seen in Table 2, in agreement with [11] who reported a 7–30% difference, and is on average around 15% across the r/T locations considered. The broadening of the turbulence levels is generally more pronounced, around 20%, in the impeller stream and in radial locations with low turbulence levels like $r/T > 0.25$. To quantify the broadening of the r.m.s. velocity due to the combined effect of macro-instabilities and periodic component the percentage error was defined as

$$\%\varepsilon_{(MI+BPF)} = \frac{u'_t - (u'_t - u'_{BPF}u'_{MI})}{(u'_t - u'_{BPF}u'_{MI})} \times 100\% \quad (2)$$

Table 2
Mean velocity and turbulence level results for PBT at $z/T = 0.27$

r/T	V	u'_t	u'_{MI}	$u'_t - u'_{MI}$	$u'_t - u'_{BPF} - u'_{MI}$	$\%\varepsilon_{MI}$	$\%\varepsilon_{(MI+BPF)}$
0.06	0.771	0.271	0.147	0.221	0.219	22.74	24
0.13	0.769	0.457	0.210	0.385	0.379	18.53	20.43
0.17	0.251	0.322	0.085	0.305	0.278	6	16.88
0.20	0.227	0.204	0.064	0.188	0.188	8	8
0.25	0.192	0.144	0.057	0.126	0.126	13.8	13.8
0.3	0.140	0.140	0.062	0.116	0.116	20	20
0.35	0.048	0.154	0.065	0.130	0.130	18.7	18.7
0.40	−0.140	0.162	0.067	0.138	0.138	17.3	17.3

Table 3
Mean velocity and turbulence level results for PBT along the main circulation loop

x/T	V	u'_t	u'_{MI}	$u'_t - u'_{MI}$	$u'_t - u'_{BPF} - u'_{MI}$	$\%\varepsilon_{MI}$	$\%\varepsilon_{(MI+BPF)}$
0.025	1.012	0.311	0.107	0.285	0.261	10	19
0.075	0.737	0.380	0.139	0.344	0.322	10.5	18.15
0.23	0.419	0.285	0.085	0.266	0.266	7.2	7.2
0.45	−0.123	0.157	0.057	0.140	0.140	12.5	12.5
0.58	−0.140	0.162	0.067	0.138	0.138	17.38	17.38
0.93	0.443	0.131	0.061	0.110	0.102	19	29.31

and accounted for an error of 8–24% in the characterisation of real turbulence (Table 2).

However, as the above results refer to a profile that crosses both the impeller stream and the upflowing stream near the wall, it is more appropriate to ascertain the corresponding variation along the PBT circulation loop. Measurements were therefore made along the centreline of the circulation loop, i.e. along a curved trajectory (denoted as x) starting below the impeller and following the path of the mean flow to the top of the impeller. The total error in turbulence estimation varies from 7–30% along the circulation loop and is more pronounced in regions close to the impeller (Table 3), while the corresponding error due to the MI contribution is around 7–19%.

The above results indicate clearly that the broadening of the measured r.m.s. levels can be as high as 20% in some locations due to the macro-instability contribution alone, and up to 30% when both the MI and the blade passing frequency contributions are included. Predictions of the flows should therefore take into account such broadening and although this may not be relevant for RANS predictions, the exclusion of such effects and of their importance for mixing process reported by Guillard et al. [26] and others will not be accounted for.

The preceding sections have indicated three important findings. First, the determination of f' values must be made with great care and comparisons between the turbulence content of different flows should only be made if appropriate time-resolved recordings have been made to enable the removal of the BPF and MI contributions to the measured r.m.s. values. This necessitates the acquisition of long recordings at high data rates and careful spectral analysis, which should be undertaken in future work for a range of vessel and impeller geometries. Second, the MI phenomenon and the corresponding f' values are affected by the *Re* of the flow, especially near the top of the vessel and this must be taken into account, especially as the volume above a certain elevation in stirred tanks is not actively involved in the mean circulation, even though there is exchange between this volume and the rest of the tank due to MIs in the flow field (Bruha et al. [7], Bittorf and Kresta [15]). The PIV data presented showed that indeed f' values are affected in that region and only for the highest *Re*s a single f' value is found. Importantly, such high *Re* values may not be reached in many vessels in practice without significant air entrainment from the free surface. Third, in view of the possible differences in flow regime and/or extent of active circulation in a stirred tank, the distribution of mean velocities near the top of the tank may affect the circulation of the precessing vortex and thus the f' values obtained. This is considered further in the following section.

3.5. Effect of impeller diameter, number of blades and number of baffles on mean flow with Rushton turbine

The findings of previous studies (e.g. Haam et al. [19]), as well as the flow visualisation observations carried out in this work, have provided evidence that the MI phenomenon is associated with a precessing vortex near the surface and is affected by interactions with the flow emerging from the baffles. Guillard et al. [20] have also argued that it is reasonable that the vortex is unstable in time and in space due to the sharp variations in pressure and inertia forces near the baffle, while Chapple and Kresta [27] have shown that the near-baffle region of the tank is characterised by strong flow direction instabilities. The most characteristic mean velocity component in respect to the above considerations is the tangential one and if its distribution for different vessel/impeller characteristics near the surface scales with V_{tip}, or equivalently N, then it might be expected that the frequency of the MI does as well. To investigate this, the tangential velocities with different numbers of blades, baffles and impeller diameters were examined in that region in the 400 mm vessel system in which changes of vessel internals could be readily achieved. However, f' measurements were not obtained due to data rate limitations and they should be studied in future work. Instead, scaling rules between the recorded velocities and the number of baffles, blades and impeller diameter were sought through measurement of the precessing vortex velocities, most pronounced near the top of the vessel, via the acquisition of mean tangential component data in that region. The rationale for this part of the work was the linearity between f and N in stirred tanks established by Nikiforaki et al. [14] for higher Res and the expectation from work in simpler configurations (for example by Vladimirov et al. [28]) that precession frequencies in general scale with rotational speed. The Rushton turbine was selected in preference to a PBT for this part of the work, as the flowfields with different impeller sizes, etc. are likely to be more similar, whereas the discharge angle for a PBT changes with

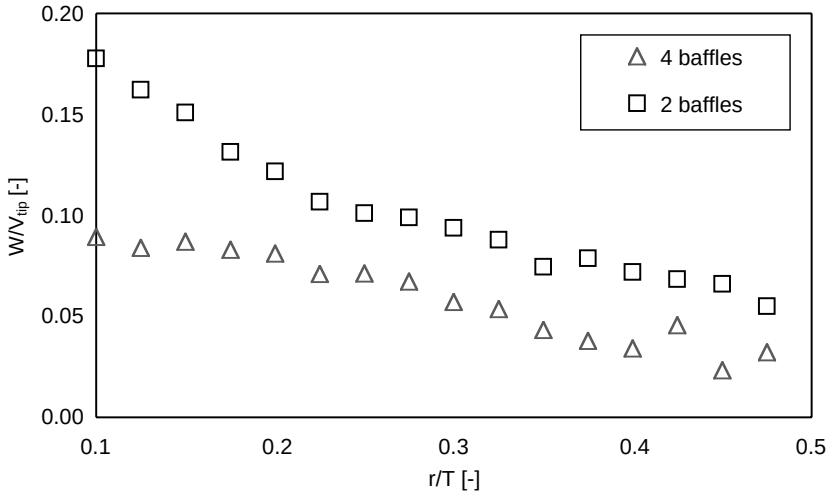

Fig. 9. Ensemble-averaged tangential mean velocity profiles near the top of the vessel with 2 and 4 baffles. Rushton turbine, $T = 400$ mm, $C/T = 0.33$, $D/T = 0.33$, $z/T = 0.95$, $Re = 5400$ and 4500 for 4- and 2-baffles cases, respectively.

Re (Hockey and Nouri [5]) and *D*/*T* (Bittorf and Kresta [15]).

LDA measurements were made in the 400 mm vessel stirred by a RT ($D/T = 0.33$, $C/T = 0.33$) with both 2 and 4 baffles. These can be seen in Fig. 9 where the normalised ensemble-averaged tangential mean velocity profiles at $z/T = 0.95$ are shown. It can be seen that with 2 baffles the normalised velocities are higher. Although the normalised velocities around $r/T = 0.1$ nearly double with the decrease in baffling, there is no evidence of scaling with the number of baffles across the entire profile. A region characterised by $W = C/r$ is evident for the 2-baffle case for $0.1 < r/T < 0.2$, but the corresponding profile is much more uniform for the 4-baffle case. Clearly, higher velocities (and a more intense surface vortex) might be expected with fewer baffles, but the lack of scaling between the two profiles indicates that the change in flow pattern involves more complex processes than a simple increase in rotational velocity with a decreasing number of baffles. Consequently, more extensive study of both the effect of *Re* and baffle number on the f' values and precessional velocities is necessary to understand the associated flow mechanisms affecting MIs.

In order to investigate whether the number of RT blades affected the measured tangential velocities, LDA measurements were made with RTs with 2, 3, 4 and 6 blades in the 400 mm vessel at $Re = 5000$–6000, again at $z/T = 0.95$. The normalised tangential velocities shown in Fig. 10 again did not scale with tip speed but in general increased with blade number. The increase in tangential velocity near the vessel surface with a reduction of baffling or an increase in blades is reasonable and might be expected. However, once more the lack of scaling prevents drawing any firm conclusions on the effect of such parameters on precessional velocities and it should be ascertained whether these influence the

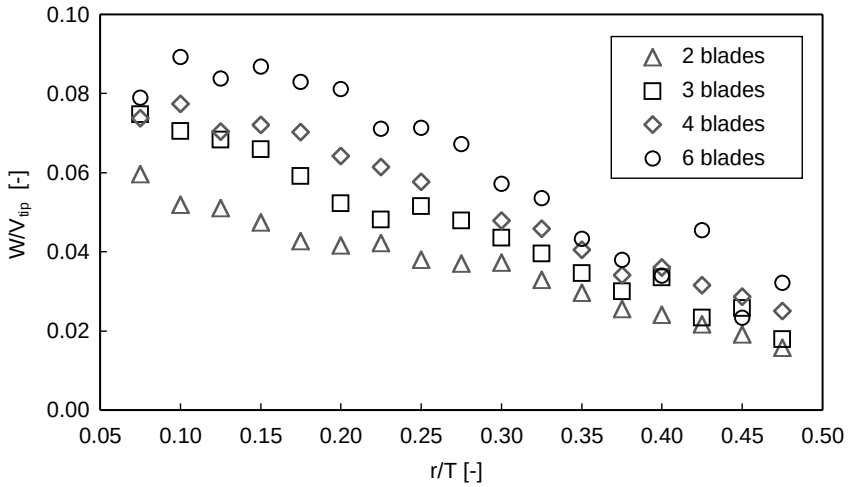

Fig. 10. Ensemble-averaged tangential mean velocity profiles near the top of the vessel with 2, 3, 4 and 6 blades. Rushton turbine, $T = 400$ mm, $C/T = 0.33$, $D/T = 0.33$, $z/T = 0.95$, $Re = 5400$.

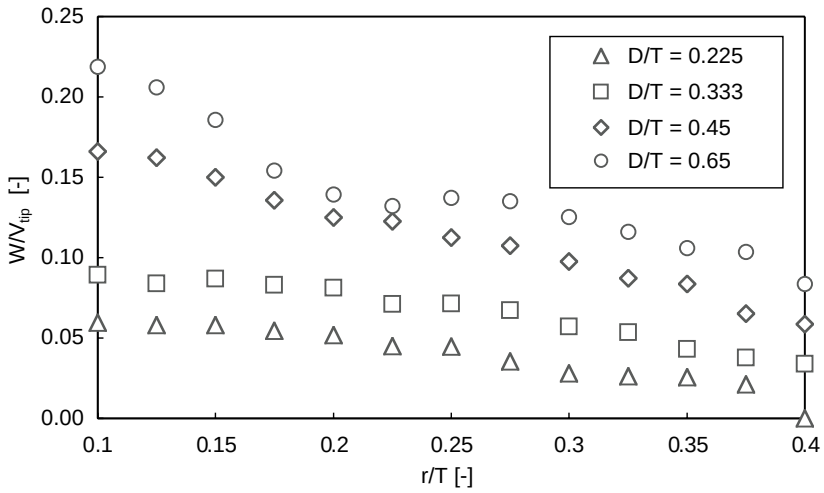

Fig. 11. Ensemble-averaged tangential mean velocity profiles near the top of the vessel with different impeller diameters. Rushton turbine, $T = 400$ mm, $C/T = 0.33$, $z/T = 0.95$. D/T= 0.225, 0.33, 0.45 and 0.65, and $Re = 5100$, 5400, 5000 and 6000, respectively.

macroinstability phenomena. Any explanation should take into account the possible generation of different number of precessing vortices when the baffle and/or blade number are altered. These issues are considered further below.

The effect of RT diameter on the mean velocities was studied through measurements obtained in the 400 mm vessel at $Re = 5000$–6000 with impellers of $D/T = 0.225$, 0.33, 0.45 and 0.65. A variation of velocities with different impeller diameters has been observed previously by Nouri et al. [29] for $Re = 8000$–$48{,}000$, but their findings were primarily concerned with the region near the impeller, where scaling was possible for turbulent *Re*s, provided that normalised spatial coordinates were employed to account for the different impeller sizes. The present data, shown in Fig. 11 for the four diameter impellers again for $z/T = 0.95$, do not scale with V_{tip}. An increase of the normalised velocity with diameter is evident, but this is not proportional to D/T.

The results presented earlier in this section have shown no clear evidence of scaling of normalised velocities with the vessel/impeller internal changes studied. This might be considered contrary to expectations and it is worthwhile examining possible reasons for the lack of scaling of the tangential velocities with rotational speed or blade tip speed. Although, as shown for example by Yianneskis et al. [22], the flow near a rotating impeller can be analysed by subtracting from the local time or phase-averaged tangential velocities the forced vortex component (i.e. $W = wr$), in any system driven by a rotating body, the flow away from that body in the tangential direction is akin to an irrotational vortex (Massey [30]), i.e. $W = C/r$. Consequently, near the top of the vessel, the local time-averaged velocities should be the resultant of the observed precessing vortex and the local "irrotational vortex" flow. It is this resultant that the present tangential velocity profiles show and, as they do not scale with *N*, this may be caused by the strength of the "irrotational vortex" flow varying with geometrical parameters such as baffle and blade number, whereas the precessing vortex component may indeed scale with *N*, or vice versa. This should be ascertained in future work through time-resolved measurements in the vicinity of the free surface. Importantly, it should also be established whether more than one vortex is present for different baffle/blade number cases, as it has only been assumed so far that a single vortex is present, based on from the standard configuration observations of Haam et al. [19] and Yianneskis et al. [22].

In addition, for all three parameters (baffle, blade number and impeller size), the findings may be complicated further by the fact that locally the flow may be predominantly transitional. Consequently, this result, in conjunction with the corresponding of Bittorf and Kresta [15] on the extent of turbulent flow in stirred tanks, indicates that, at least for the low *Re* cases in the RT-stirred vessels studied, the flows away from the impeller blades may be affected by the locally not fully turbulent flow regime. An important corollary of these observations is that scaling in stirred tanks may be far more complex than a simple comparison of normalised mean and/or r.m.s. velocities may indicate, and that any such comparisons should be made with extreme care.

In relation to the above, the relation between *Re* and extent of laminar/turbulent flow in a stirred vessel is not well established for different scales. The present work indicated that, at least in terms of f', a change occurs at *Re* around 16,000–20,000 and this change is essentially completed when *Re* has reached 40,000. Hasal et al. [10] reported f' values of 0.06 for $Re = 75{,}000$, and 0.09 for $Re = 750$ and 1200, in a vessel stirred by a PBT. Although a value of $Re > 20{,}000$ is normally cited for turbulent flow in a tank, the manner of transition to turbulent flow appears rather complex and poorly understood. For example, Kemoun et al. [31] have found a linear increase in the r.m.s. levels for $Re > 260$ in an oil-filled tank and in the shear stresses levels for $Re > 30{,}000$ in a water-filled system. Montes et al. [8]

found a sudden increase in normalised r.m.s. levels for $Re > 500$, while Schäfer et al. [21] found that with a PBT turbulence levels scaled with N for $Re > 5000$. Clearly, a more thorough assessment of the state of the flows is needed.

The flows in stirred tanks are rather more complex, but some insight can be provided by the findings of Vladimirov et al. [28] who studied the effect of various geometrical parameters on precessing structures in simple rotating flows. Vladimirov et al. found that for a wide range of flows driven by rotating bodies of different shapes precessing structures were present, whose precession rate was linearly related to the rotational speed. The f' in their propeller-driven flow was proportional to their parameter equivalent to the present D/T when the latter assumed values greater than 0.1. Although direct comparisons are clearly not possible, their work and the substantial efforts made to date to understand MI phenomena in stirred vessels, may point to the potential benefits that a carefully planned sequence of experiments in less complex geometries could provide for an improved understanding of such instabilities. The precessional MI is a true flow instability that is encountered in most, if not all, swirling flows, albeit to different extent and/or with different magnitudes; indeed the precessing vortex core may travel in the same or the opposite direction to that of the flow rotation, or be stationary for some flow conditions (Vladimirov et al. [28]).

In addition, the present work has shown, in agreement with Montes et al. [8], that studying lower Reynolds numbers should help bridge a gap in the understanding and provide a more complete description of the MI phenomena and hence quantify their importance for related mixing process applications. Further work with different impeller diameters, which should also encompass low Reynolds numbers and simpler geometries, is necessary before a more unified understanding of macro-instabilities can be achieved. In particular, as an overview of the results of [12,14] in stirred tanks and of [28] in simpler geometries indicates that impeller diameter may have an effect on the MI frequencies generated by precessional motions, it would be interesting to confirm this and quantify such a dependence of f' on D/T, while the results of both [12,14] have both shown no effect of C/T on f' for the geometries studied, and therefore impeller clearance can be expected to have little effect. The experiments of [12] have also shown that fluid density and viscosity have no noticeable effect on f' and it would be useful to examine the influence of these properties for different D/T impellers. The results show conclusively that the characteristic frequencies of MIs, and consequently the time scales over which they may affect mixing and reaction phenomena, depend on impeller rotational speed and not on the geometry or fluid properties and that although f' assumes different values at low and high Re ranges, the change of f' that takes place over intermediate Re values deserves further investigation to enable harnessing such instabilities for optimisation of process design. There is clearly much research still needed to fully characterise and understand macroinstabilities in stirred tanks.

4. Concluding remarks

The LDA and PIV measurements reported here for different impeller and tank geometries have sought to improve understanding of macro-instability phenomena. The associated mechanism is rather complex, especially for the PBT, and an effort was made to provide answers or pose questions for future research, as appropriate. The large-scale motions in a stirred vessel are strongly affected by the MI and its effect on the mixing process can be significant, as r.m.s. levels, for example, may be broadened by up to 20%. This could have important implications for reaction yield in stirred tank systems, although exact quantification of the effect of MIs is fraught with difficulties; there is little work in this area but it should be noted that Houcine et al. [32] have indicated that feed stream intermittency is present in continuous stirred tank reactors which may be influenced by macro-instabilities: they identified intermittencies with periods of a few seconds that might affect macro- and meso-mixing.

Importantly, although f' was constant throughout the vessel at the highest Re values, increasingly larger regions of higher f' were detected as Re was reduced, and this may stem from the limited extent of turbulent flow across the vessel, which has been previously reported by Bittorf and Kresta [15]. In such cases, even when the mean velocities and turbulence levels scale well with blade tip speed near the impeller, perfect scaling is not found away from the blades. Measurements for low Re near the liquid surface with different impeller diameters, number of baffles and number of blades showed no simple scaling of the tangential mean velocity with blade tip speed. This may influence the precessional motion of the MI and should be investigated further to help establish scaling rules.

Care should therefore be exerted when extrapolating results from low to high Re flows, especially as it may be unlikely that fully turbulent flow conditions can be achieved in many vessels before significant air entrainment from the free surface, with all the associated complicating influences, commences. The preceding considerations for the region near the top of the vessels may also apply to multiple-impeller tanks, when the impeller spacing is relatively large and the circulation loops do not interact, as for example, in the “parallel” flow of Rutherford et al. [3] with two Rushton impellers.

Suitably-designed experiments in stirred vessels with low Reynolds numbers, different impeller diameters and simpler geometries should help throw light into the complex phenomena involved.

Acknowledgements

The authors acknowledge support by the E.U. under the Growth Programme project “Optimisation of Industrial Multiphase Mixing” GRD1-2000-25359.

References

[1] S. Kresta, Turbulence in stirred tanks: anisotropic, approximate and applied, Can. J. Chem. Eng. 76 (1998) 563–576.

[2] S. Kresta, P.E. Wood, The mean flow pattern produced by a 45° pitched blade turbine: changes in the circulation pattern due to off bottom clearance, Can. J. Chem. Eng. 71 (1993) 42–53.

[3] K. Rutherford, S.M.S. Mahmoudi, K.C. Lee, M. Yianneskis, Hydrodynamic characteristics of dual Rushton impeller stirred vessels, Am. Inst. Chem. Eng. J. 42 (1996) 332–346.

[4] G. Montante, K.C. Lee, A. Brucato, M. Yianneskis, Double- to single-loop flow pattern transition in stirred vessels, Can. J. Chem. Eng. 77 (1999) 649–659.

[5] R. Hockey, J.M. Nouri, Turbulent flow in a baffled vessel stirred by a 60° pitched blade impeller, Chem. Eng. Sci. 19 (1996) 4405–4421.

[6] M.F.W. Distelhoff, A.J. Marquis, J.M. Nouri, J.H. Whitelaw, The application of a strain gauge technique to the measurement of power characteristics of impellers, Exp. Fluids 20 (1995) 56–58.

[7] O. Bruha, I. Fort, P. Smolka, Phenomenon of turbulent macro-instabilities in agitated systems, Collect. Czech. Chem. Commun. 60 (1995) 85–94.

[8] J.-L. Montes, H.-C. Boisson, I. Fort, M. Jahoda, Velocity field macro-instabilities in an axially agitated mixing vessel, Chem. Eng. J. 67 (1997) 139–145.

[9] K.J. Myers, R.W. Ward, A. Bakker, A digital particle image velocimetry investigation of flow field instabilities of axial-flow impellers, ASME J. Fluids Eng. 119 (1997) 623–632.

[10] P. Hasal, J.-L. Montes, H.-C. Boisson, I. Fort, Macro-instabilities of velocity field in stirred vessel: detection and analysis, Chem. Eng. Sci. 55 (2000) 391–401.

[11] V.T. Roussinova, B. Grgic, S.M. Kresta, Study of macro-instabilities in stirred tanks using a velocity decomposition technique, Trans. I. Chem. E 78 (A) (2000) 1040–1052.

[12] V. Roussinova, S.M. Kresta, R. Weetman, Low frequency macroinstabilities in a stirred tank: scale-up and prediction based on large eddy simulations, Chem. Eng. Sci. 58 (2003) 2297–2311.

[13] O. Bruha, I. Fort, P. Smolka, M. Jahoda, Experimental study of turbulent macro-instabilities in an agitated system with axial high-speed impeller and radial baffles, Collect. Czech. Chem. Commun. 61 (1996) 856–867.

[14] L. Nikiforaki, G. Montante, K.C. Lee, M. Yianneskis, On the origin, frequency and magnitude of macro-instabilities of the flows in stirred vessels, Chem. Eng. Sci. 58 (2003) 2937–2949.

[15] K. Bittorf, S. Kresta, Active volume of mean circulation for stirred tanks agitated with axial impellers, Chem. Eng. Sci. 55 (2000) 1325–1335.

[16] S. Baldi, D. Hann, M. Yianneskis, On the measurement of turbulence energy dissipation in stirred vessels with PIV techniques, in: Proceedings of the 11th International Symposium on Applications of Laser Techniques to Fluid Mechanics, Lisbon, July 2002.

[17] J. Yu, Air entrainment and macro-instability in stirred vessels, Ph.D. thesis, Friedrich-Alexander-Universität Erlangen-Nürnberg, Erlangen, Germany, 2003.

[18] G. Zhou, Ph.D. thesis, Characteristics of turbulence energy dissipation and liquid–liquid dispersions in an agitated tank, University of Alberta, Canada, 1996.

[19] S. Haam, R.S. Brodkey, J.B. Fasano, Local heat transfer in amixing vessel using heat flux sensors, Ind. Eng. Chem. Res. 31 (1992) 1384–1391.

[20] F. Guillard, C. Tragardh, L. Fuchs, A study of turbulent mixing in a turbine-agitated tank using a fluorescence technique, Exp. Fluids 28 (2000) 225–235.

[21] M. Schäfer, M. Yianneskis, P. Wächter, F. Durst, Trailing vortices around a 45° pitched blade impeller, AIChE J. 44 (1998) 1233–1246.

[22] M. Yianneskis, Z. Popiolek, J.H. Whitelaw, An experimental study of the steady and unsteady flow characteristics of stirred reactors, J. Fluid Mech. 175 (1987) 537–555.

[23] T. Kovács, C. Trägård, L. Fuchs, Fourier spectrum to recover deterministic and stochastic behaviour in stirred tanks, AICHE J. 47 (10) (2001) 2167–2176.

[24] R. Hockey, Ph.D. thesis, Turbulent Newtonian and non-Newtonian flows in a stirred reactor, University College London, University of London, 1990.

[25] B. Grgic, M.Sc. thesis, Influence of the impeller and tank geometry on low frequency phenomena and flow instability, University of Alberta, Canada, 1998.

[26] F. Guillard, C. Tragardh, L. Fuchs, A study on the instability of coherent mixing structures in a continuously stirred tank, Chem. Eng. Sci. 55 (2000) 5657–5670.

[27] Chapple, Kresta, The effect of geometry on the stability of flow patterns in stirred tanks, Chem. Eng. Sci. 21 (1994) 3651–3660.

[28] V.A. Vladimirov, V.I. Yudovich, M.Y. Zhukov, P.V. Denissenko, Asymmetric flows induced by a rotating body in a thin layer, HIMSA report, University of Hull, 2001.

[29] J.M. Nouri, J.H. Whitelaw, M. Yianneskis, The scaling of the flow field with impeller size and rotational speed in a stirrred reactor, in: Proceedings of the Second International Conference on Laser Anemometry—Advances and Applications, Glasgow, Springer-Verlag, 21–23 September 1987, pp. 489–500.

[30] B.S. Massey, Mechanics of Fluids, Chapman Hall, London, 1990.

[31] A. Kemoun, F. Lusseyran, J. Mallet, M. Mahouast, Experimental scanning for simplifying the model of a stirred-tank flow, Exp. Fluids 25 (1998) 23–36.

[32] I. Houcine, E. Plasari, R. David, J. Villermaux, Feedstream jet intermittency phenomena in continuous stirred tank reactor, Chem. Eng. J. 72 (1998) 19–30.